Ion Channels in Small Cells and Subcellular Structures Can Be Studied with a Smart Patch-Clamp System

Julia Gorelik,* Yuchun Gu,* Hilmar A. Spohr,* Andrew I. Shevchuk,* Max J. Lab,[†] Sian E. Harding,[†] Christopher R. W. Edwards,[‡] Michael Whitaker,[‡] Guy W. J. Moss,[§] David C. H. Benton,[§] Daniel Sánchez,[¶] Alberto Darszon,[¶] Igor Vodyanoy,[∥] David Klenerman,** and Yuri E. Korchev*

*Division of Medicine and [†]National Heart and Lung Institute, Imperial College of Science, Technology and Medicine, MRC Clinical Sciences Centre, London W12 0NN, United Kingdom; [‡]Department of Physiological Sciences, University of Newcastle, Newcastle upon Tyne, United Kingdom; [§]Department of Pharmacology, University College London, London, United Kingdom; [¶]Department of Development Genetics and Molecular Physiology, Institute of Biotechnology, National Autonomous University of Mexico, Cuernavaca, Morelos, Mexico; [∥]Office of Naval Research, Arlington, Virginia USA; and **Department of Chemistry, Cambridge University, Cambridge, United Kingdom

ABSTRACT   We have developed a scanning patch-clamp technique that facilitates single-channel recording from small cells and submicron cellular structures that are inaccessible by conventional methods. The scanning patch-clamp technique combines scanning ion conductance microscopy and patch-clamp recording through a single glass nanopipette probe. In this method the nanopipette is first scanned over a cell surface, using current feedback, to obtain a high-resolution topographic image. This same pipette is then used to make the patch-clamp recording. Because image information is obtained via the patch electrode it can be used to position the pipette onto a cell with nanometer precision. The utility of this technique is demonstrated by obtaining ion channel recordings from the top of epithelial microvilli and openings of cardiomyocyte T-tubules. Furthermore, for the first time we have demonstrated that it is possible to record ion channels from very small cells, such as sperm cells, under physiological conditions as well as record from cellular microstructures such as submicron neuronal processes.

INTRODUCTION

The patch-clamp technique, first described by Neher and Sakmann (Neher and Sakmann, 1976; Neher et al., 1978) and initially refined by Hamill (Hamill et al., 1981) is the main experimental approach used for obtaining information about the characteristics and distribution of ion channels in living cells. Some variations of this technique have since been developed for specific experimental situations (Levitan and Kramer, 1990; Jonas et al., 1997), and together these methods have allowed recording in an enormous variety of situations. Data from this type of experiment, along with a host of other work, have shown that ion channels frequently associate with specific subcellular structures and are not uniformly distributed on the cell surface; this is important for their function (Joe and Angelides, 1992; Angelides, 1986; Banke et al., 1997; Alkondon, 1996; Tousson et al., 1989; Frosch and Dichter, 1992; Kinnamon et al., 1988; Karpen et al., 1992; Cohen et al., 1991; Gu et al., 2002; Korchev et al., 2000a) However, the available methods remain limited when it comes to studying this subcellular distribution of channels. For example, it is still difficult to record from fine structures such as microvilli and the fine dendritic branches of neurons or to patch opaque samples or obscured structures such as transverse tubules from muscle. A major reason for this is the difficulty in controlling patch pipettes in their approach to such samples. This is because an electrode is typically positioned using manual adjustments while focusing between the pipette and sample under a light microscope. Some samples, such as transverse tubules, are not optically visible so these present inherent difficulty. Ultra-fine structures also provide a considerable challenge because high-magnification objectives with a short depth of field are used so that for much of the pipette approach, sample and electrode are not in the same focal plane. Under these circumstances it is easy to damage the pipette tip.

In this study we demonstrate the utility of a new patch-clamp method that solves these problems and enables both the identification of small cellular or subcellular membrane structures as well as subsequent patch recording. Our method combines the capabilities of conventional patch clamping with the advanced features of scanning ion conductance microscopy (SICM) (Hansma et al., 1989). SICM allows both ultra-fine positioning of the probe over the sample and high-resolution imaging of living cell membranes (Korchev et al., 1997, 2000b; Shevchuk et al., 2001). Because the SICM probe is also used as the patch pipette, it provides its own image of the cell surface and ensures precise positioning of the electrode relative to the cell topography. The development of this method thus allows the investigation of ion channels that have a unique spatial distribution in otherwise difficult samples and may also lead to new methods for automated patch recording.
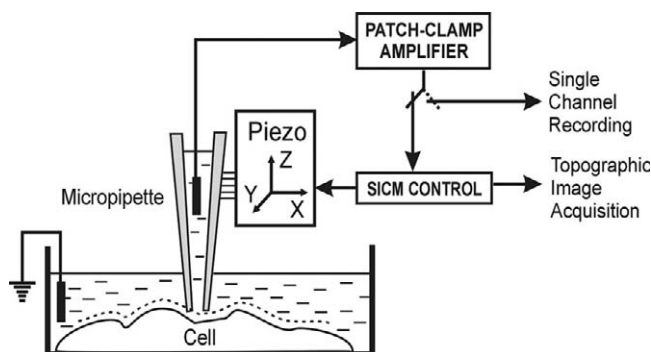
FIGURE 1 Schematic diagram of the scanning patch-clamp setup. The micropipette is mounted on a three-axis piezo actuator controlled by a computer. The ion current that flows through the pipette is measured by a patch-clamp amplifier, and it is used for the feedback control to keep a constant distance between the micropipette and the sample during scanning. Upon completion of the scanning procedure, computer control is used to position the micropipette at a place of interest based on the topographic image acquired, and finally the same patch-clamp amplifier is used for electrophysiological recording.

MATERIALS AND METHODS

Operation of the scanning patch-clamp is based on the idea that both SICM and patch-clamp recording use a glass micropipette as their probe. By combining these techniques the same micropipette can be used first in SICM protocols to image the cell surface and identify membrane structures of interest and then as a patch pipette for electrophysiological recording as shown schematically in Fig. 1. In this method the scanning micropipette is arranged vertically and manipulated by SICM computer control (Fig. 2 *A*). A feedback control system is in operation while the pipette approaches the cell surface. As soon as the pipette reaches a distance *d* from the surface, the SICM feedback control maintains a constant tip-sample separation. This procedure makes the approach straightforward and safe, because the patch pipette is prevented from touching the cell membrane until it is desired to do so to form a seal. It is important to note that a visual image of the sample is not necessary for this approach. Once the SICM protocol has obtained a topographic image of the cell surface it can be used to position the patch pipette over an exact place of interest for patch recording (Fig. 2 *B*). Finally, feedback control is switched off, the pipette is lowered, and suction is applied, resulting in the formation of a gigaohm seal (Fig. 2 *C*). Ion channel recording is then performed by conventional methods with all configurations available, e.g., cell-attached, inside-out, whole-cell, and/or outside-out mode.

Instrument

The basic topographic imaging equipment is as previously described for the SICM method (Korchev et al., 1997). Briefly, the pipette is filled with electrolyte and mounted on a piezo stage that is moved over the cell while maintaining it at a fixed distance from the surface (Figs. 1 and 2). This is achieved by a distance-modulated feedback control (Shevchuk et al., 2001) designed to keep a constant ion current flowing through the pipette. The present instrument is based on an inverted optical microscope (Diaphot 200, Nikon Corp., Tokyo, Japan) with a mechanism for coordinating optical and scanned images, through a video camera with frame-grabbing hardware and software. There is a computer-controlled three-axis translation stage with measurement and feedback systems (East Coast Scientific, Cambridge, UK), which scans the micropipette tip over the specimen. For living cells, displacements in excess of 30–50 μm in the vertical direction are required. We have, therefore used a three-axis piezo translation stage
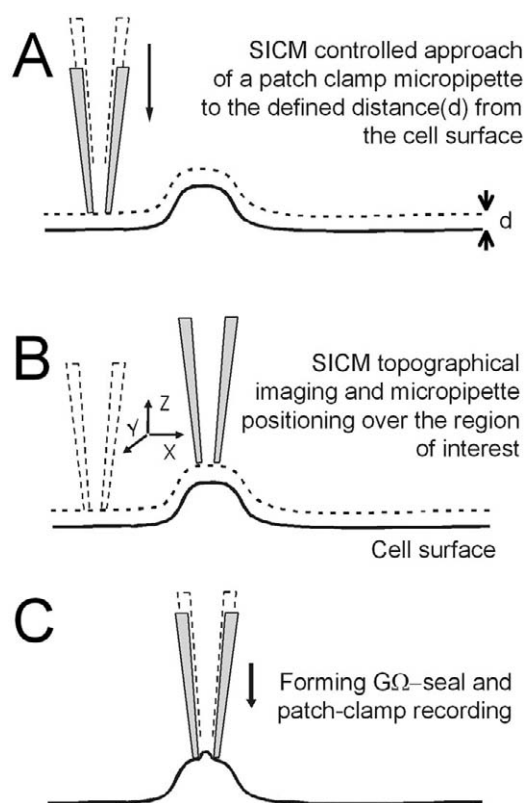

FIGURE 2 Scanning patch-clamp principle of operation. (*A*) A micropipette approaches the cell surface and reaches a defined separation distance (*d*) whereupon the distance is kept constant by SICM feedback control. (*B*) The SICM scans this micropipette over the cell surface and positions it at a place of interest for patch-clamp recording. (*C*) The micropipette is lowered to form the gigaohm seal for patch-clamp recording from the selected structure.

(Tritor, Piezosystem Jena, Germany) with a 100-μm travel distance in the *x*, *y*, and *z* directions.

This setup was adapted for high-resolution patch clamping by replacing the current amplifier used previously with a commercial patch-clamp amplifier (Axopatch 200B, Axon Instruments, Foster City, CA). Nanopipettes were made from 1.00-mm outer diameter and 0.58-mm inner diameter borosilicate glass capillaries (Intracel, Herts, UK) using a laser-based puller (P-2000, Sutter Instrument Co., San Rafael, CA). Pipettes were used without any further treatment such as fire polishing or Sylgard coating. The pipette tip radius, determined by scanning electron microscopy, was ∼100 nm and when filled with pipette solution had an average tip resistance of 150 MΩ. For patch-clamp recording, currents were sampled at 10 kHz and filtered at 2 kHz (−3 dB, 4-pole Bessel) using an Axopatch 200B amplifier and pClamp 8.0 software (Axon Instruments), which was also used to generate pulse protocols.

Cell preparations and solutions for patch-clamp recording

Sperm

Strongylocentrotus purpuratus or *Lytechinus pictus* sea urchins were obtained from Pacific Bio-Marine Laboratories (Long Beach, CA). Spermatozoa were obtained by intracoelomic injection of 0.5 M KCl into sea urchins and collected with a Pasteur pipette directly from the gonopores (Lee and Garbers, 1986). The cell suspension was kept on ice in physio-

logical bath solution composed of (mM) 486 NaCl, 10 KCl, 25 $MgCl_2$, 10 $CaCl_2$, 10 HEPES, pH 8. Cells were pretreated with 0.01 mg/ml trypsin (Sigma, Poole, UK) solution during 10 min in ice and plated on poly-L-lysine-treated dishes in physiological bath solution. Pipette filling solution contained (mM) 300 $BaCl_2$, 10 HEPES, pH 8.0.

Neurons

Superior cervical ganglion cells were cultured from 17-day-old Sprague-Dawley rats using previously described methods (Dunn, 1994). Briefly, ganglia were dissociated with collagenase followed by trypsin and were cultured in L-15 medium supplemented with 10% fetal calf serum and 50 ng/ml nerve growth factor. To investigate the calcium channels, the bath solution was composed of (mM) 120 KCl, 3 $MgCl_2$, 5 EGTA, 11 glucose, 10 HEPES, adjusted to pH 7.4 with KOH, and the pipette solution contained 90 $BaCl_2$, 10 HEPES, 10 tetraethylammonium(TEA)-Cl, 3 4-aminopyridine (4-AP), adjusted to pH 7.4 with TEA-OH, as described previously (Delmas et al., 2000). To investigate K^+ channels, Leibovitz's L-15 medium was used. In several experiments we loaded the cells with DiI as previously described (Hasbani et al., 2001).

Cardiac myocytes

Left ventricular cells from the rat myocardium were isolated as previously described (Harding et al., 1988). Cells were allowed to attach to polystyrene cell culture dishes filled with bath solutions composed of (in mM) 120 K-glutamate, 25 KCl, 2 $MgCl_2$, 1 $CaCl_2$, 2 EGTA, 10 glucose, 10 HEPES, adjusted to pH 7.4 with NaOH for the Ca^{2+} experiments. Pipette filling solutions were composed of (in mM) 70 $BaCl_2$, 10 HEPES, 110 sucrose, adjusted to pH 7.4 with TEA-OH for the Ca^{2+} experiments. Ionic compositions were similar to those previously used (Fan et al., 2000). Experiments were started after cells ceased to contract due to depolarization by high $[K^+]_{bath}$.

Epithelial kidney cells

A single A6 cell line was kindly provided by Dr. DeSmet. All experiments were carried out on cells between 127 and 134 passages. Cells were cultured as described previously (Sariban-Sohraby et al., 1984) on high-pore-density membrane filters (Falcon, Bedford, MA). Cells were grown and kept in a 1:1 mixture of modified Ham's F-12 medium and Leibovitz's L-15 medium, modified to contain 105 mM NaCl and 25 mM $NaHCO_3$. The mixture was supplemented with 10% fetal calf serum, 200 μg/ml streptomycin, and 200 U/ml penicillin. Cells were maintained at 28°C in an atmosphere of humidified air plus 1% CO_2. Cells were passaged and used between days 4 and 5 when they were 90–95% confluent. Single-channel recordings were performed using a bath solution and pipette backfill solution both composed of (in mM) 140 NaCl, 5 KCl, 0.8 $MgCl_2$, 1.2 $CaCl_2$, 10 HEPES, pH 7.4.

Aorta

Samples of aorta obtained from male Sprague-Dawley rats, 200–300 g, were kindly provided by Susan Nourshargh (Imperial College, London). The aorta was mounted in a petri dish and imaged in Leibovitz's L-15 medium.

RESULTS AND DISCUSSION

The key feature of our method is a patch electrode that first gathers topographic information and can then be used to seal onto the cell at a precise location. For this reason we

call the method smart patch. To explore the potential of this smart-patch technique we chose various experimental conditions and artificially divided them into three groups: first, small samples, visible optically but patched under feedback control; second, samples that are too small to be properly resolved or structures that are undetectable by light microscopy; and finally, opaque samples, where optical imaging is impossible. We show that we can make channel recordings in all of these situations.

Samples visible optically but patched with feedback control

Direct electrophysiological characterization of the ion channels in sperm by conventional patch-clamp is difficult because of their small size. In examining sea urchin sperm, previous studies have tried to get round this issue by using osmotic swelling to facilitate high-resistance seal formation. However, the cell-attached seals obtained in this fashion lasted only for a few minutes, making the characterization of ion channels difficult (Sanchez et al., 2001). As another alternative, spermatogenic cells, the progenitors of sperm that are larger, have been used to study sperm ion channel electrophysiology (Munoz-Garay et al., 2001). The disadvantage of this approach is that during the last stages of spermatogenesis the type and localization of ion channels may significantly change (Serrano et al., 1999). As a third alternative, ion channels from sperm have been reconstituted into artificial lipid bilayers. Unfortunately this type of reconstitution makes the definition of channel orientation problematic (Lievano et al., 1990).

Fig. 3 *A* shows the first direct recordings of a channel on a sea urchin's sperm using our smart-patch setup. This recording shows a voltage-dependent multi-state Ca^{2+} channel with a high main-state conductance that is similar to the multi-state conductances seen in planar bilayer recordings (Lievano et al., 1990). This recording allows us to assign the polarity of this sperm channel indicating that it opens at positive potentials and then relaxes to lower-conductance states. Such a channel may thus participate in the uptake of Ca^{2+} required for the acrosome reaction (Lievano et al., 1990). The probability of obtaining a seal on the sperm cell body using our smart-patch method is 0.45 (in a total of 40 patches), which is 15 times higher than the probability reported in previous studies using conventional patch-clamp setup (Guerrero et al., 1987). The duration of cell-attached seals was ~20 min. Also, for the first time, we managed to obtain an ion channel recording from sea urchin sperm cells in inside-out configuration.

By using infrared video microscopy and differential interference contrast optics, it is possible to obtain patch recordings from the dendrites of some neurons in slice preparations (Johnston et al., 1996; Stuart et al., 1993). However, by the methods currently available it is difficult to patch the finest dendritic processes or structures, so for
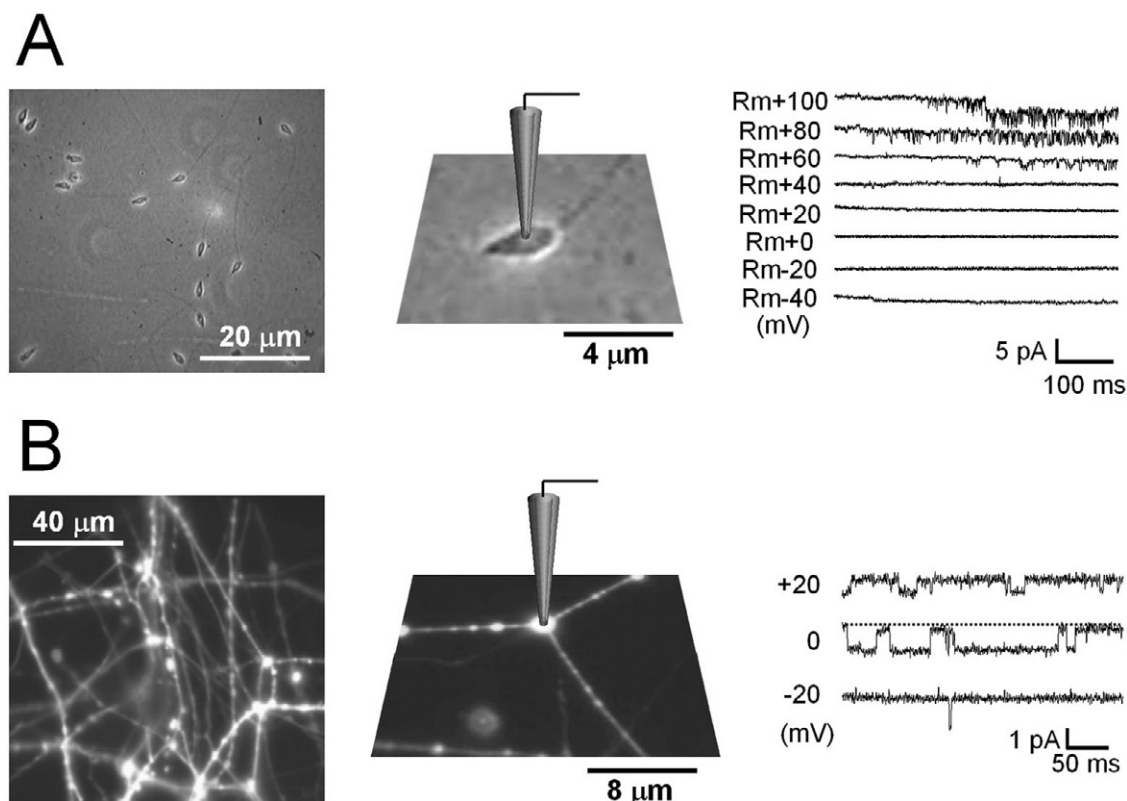
FIGURE 3   Ion channel recordings from sea urchin spermatozoa and from fine neuronal processes. (*A*) Smart patch-clamp recording from sea urchin spermatozoa: optical image of sea urchin sperm (*left*), a schematic of the pipette positioned over a sperm (*middle*), and a cell-attached current recording showing Ba^{2+} currents through Ca^{2+} channels (*right*). (*B*) Smart patch-clamp recording from a neurite varicosity structure: optical image of SCG neurites loaded with a lipid-binding dye DiI (*left*), the pipette placed above the junction between neurites (*middle*), and a cell-attached recording of Ba^{2+} currents through Ca^{2+} channels (*right*).

technical reasons, most recordings are usually made on larger features, e.g., dendrites >1 μm in diameter (Stuart et al., 1993).

Both optically and by the smart-patch technique we observed the formation of focal swellings (varicosities) on the dendrite-like structures of superior cervical ganglion (SCG) neurons in culture. These varicosities (0.5–1 μm) were visible in a light microscope and may be related to similar structures seen in organotypic slice and cultured cell preparations of central nervous system neurons where it has been demonstrated that sustained transmitter stimulation can mediate their formation (Park et al., 1996). We have patched this type of varicosity on the processes of cultured SCG neurons and found that a 22-pS cation channel is present Fig. 3 *B* (*right panel*). The current-voltage curve (data not shown) is characteristic of a calcium channel. It is perhaps surprising that with such a fine pipette we are still able to obtain channel recordings. However, conventional patch recording of channels in dendrites has shown that the calcium channels tend to cluster (Lipscombe et al., 1988), so if the right location is selected channels can be found.

Structures not clearly resolved by light microscopy

A second type of experimental sample that presents difficulties for conventional patch-clamp recording consists of those that are not clearly resolved by light microscopy. We illustrate this with a neuronal structure whose vertical dimension is too small to be properly resolved and with transverse tubules that cannot be suitably detected using light microscopy. Under these conditions the scanning patch clamp was implemented fully as described in Fig. 1; the SICM topographical image of the cell surface was acquired and then the pipette was positioned to the selected region of interest according to known coordinates.

In our first example, a flat membranous protrusion ($\sim$100 nm in height) formed on a SCG dendrite-like structure was scanned and patched. As with the neurite varicosities we were able to find channels on the surface of this structure; Fig. 4 *A* shows the recording of ion channel current. This channel was identified as a potassium channel on the basis of its reversal potential. The probability of obtaining a seal on SCG neurites was 0.62 (in a total of 29 patches).
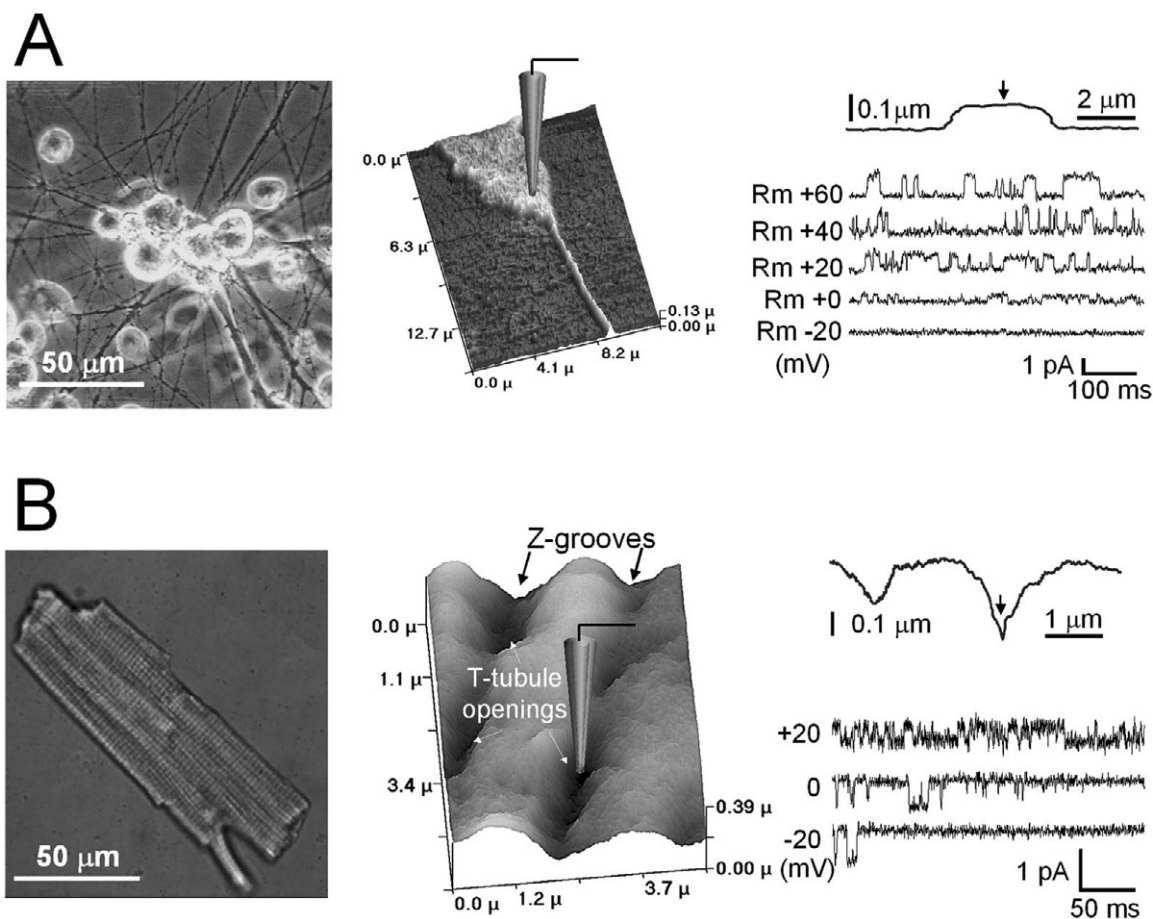
FIGURE 4   Ion channel recordings from a fine neuronal process and T-tubule opening of a cardiac myocyte. (*A*) Smart patch-clamp recording from a fine neuronal process: optical image of SCG cells (*left*), SICM image of a flat membranous protrusion formed on an SCG neurite, which is approximately 100 nm in height (*middle*), and outward K^+ currents recorded in the cell-attached configuration (*right*; *inset* shows a profile of neurite process where the position of the pipette is marked by an *arrow*). (*B*) Smart patch-clamp recording from a T-tubule opening of a cardiac myocyte: optical image of adult rat cardiomyocyte (*left*), SICM image of a rat cardiomyocyte membrane, with Z-grooves, T-tubule opening, and characteristic sarcomere units marked (*middle*), and cell-attached Ba^{2+} currents through Ca^{2+} channel (*right*; *inset* shows profile of cardiac myocyte membrane where the pipette's position is marked by an *arrow*).

The transverse tubular system of cardiac muscle is a structure that allows rapid propagation of excitation into the cell interior (Cheng et al., 1994). It has been shown by immunofluorescence and immunoelectron microscopy that L-type Ca^{2+} channels are distributed along the T-tubule membrane (Carl et al., 1995; Sun et al., 1995). However, no direct electrophysiological recordings of ion channels using conventional methods in transverse tubule opening regions have been reported to date. This is mainly because of the difficulty in visualizing transverse tubule openings using light microscopy. Furthermore, it is not possible to position the patch-clamp pipette into such small openings to obtain ion channel recordings with conventional methods. Fig. 4 *B* presents an example of ion channel patch-clamp recording in a T-tubule opening of a cardiac myocyte. This channel has the current-voltage and temporal characteristics of an L-type Ca^{2+} channel, which is to be expected in the T-tubule opening regions. Recently, we have been able to use this technique to show that the L-type Ca^{2+} and Cl^- channels are distributed and co-localized in the region of T-tubule openings, but not in other regions of the myocyte. The probability of obtaining a seal was 0.70 at the regions of the Z-groove, 0.59 at the T-tubule opening, and 0.96 at the scallop crest (Gu et al., 2002).

Nontransparent samples

Using conventional optical microscopy there is no satisfactory way to patch nontransparent samples such as intact tissues and cells grown on nontransparent material. Although it is possible to use the blind-patch approach this provides no information about the position or type of cellular structure from which a recording is made. In this study we have applied the smart-patch approach to two nontransparent samples. The first is an intact tissue preparation of rat
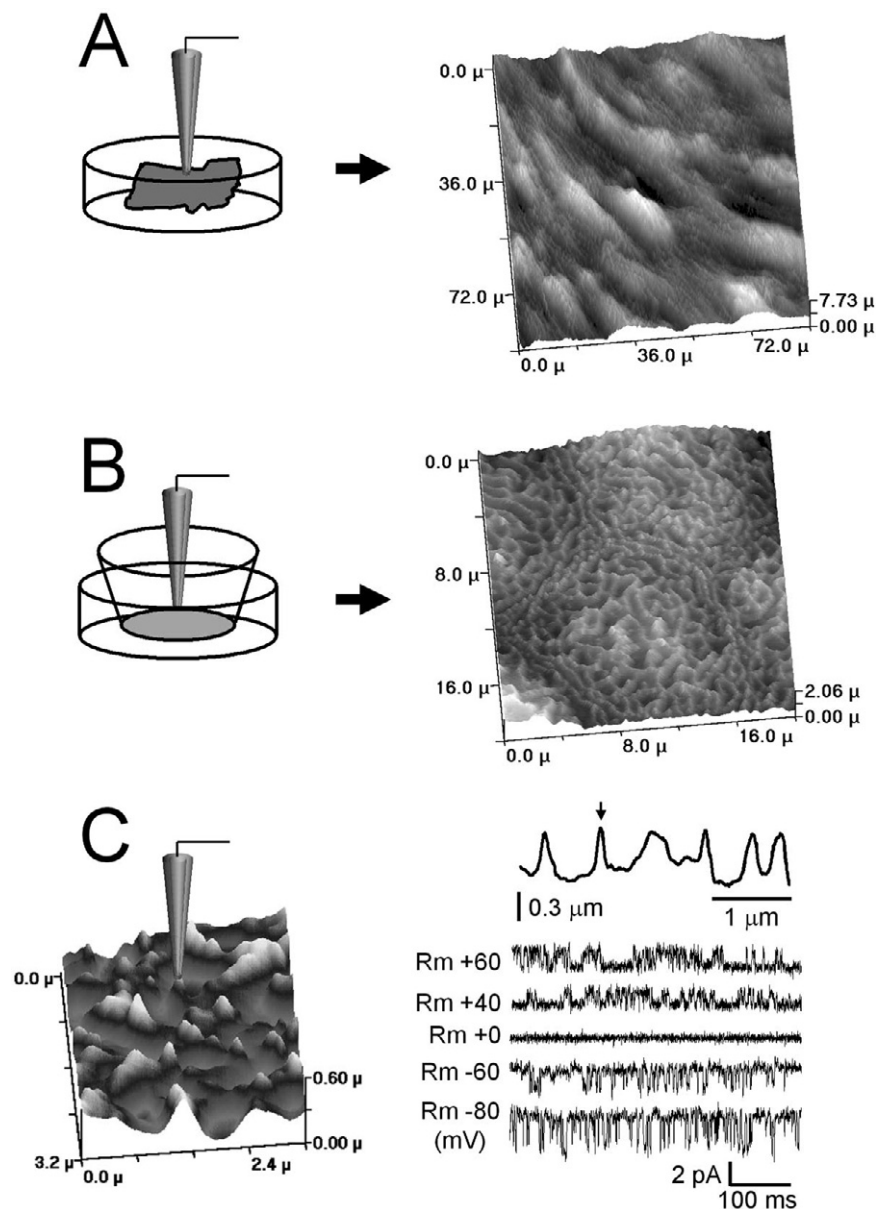
FIGURE 5 Ion channel recording from non-transparent samples. (*A*) Obtaining a SICM image of endothelial cells without optical control: schematic picture of a setup for scanning the inner surface of an opened-up rat aorta in a petri dish (*left*) and SICM image of endothelial cells of rat aorta (*right*). (*B*) Obtaining a topographic image from a nontransparent object: schematic picture of a set-up for scanning A6 epithelial cells on a non-transparent filter, which has a high pore density (*left*), and SICM image of a monolayer of A6 cells (*right*). The frame contains four epithelial cells and numerous microvilli are seen. (*C*) Ion channel recording on the top of a single microvillus: enlarged image of an A6 cell surface, where the pipette was placed on top of a microvillus (*left*) and K$^+$ channel currents recorded at the top of a microvillus in cell-attached configuration (*right*; *inset* shows the profile of several microvilli where the pipette's position is marked by an *arrow*).

aorta, and the second is a layer of A6 cells cultured on a nontransparent filter. Fig. 5 shows topographical images obtained by using the smart patch to scan the rat aortic endothelial cells (Fig. 5 *A*) and epithelial cells grown on a nontransparent filter, with high pore density (Fig. 5 *B*). With these images the patch pipette can be easily positioned at a region of interest on the cell surface and then used to obtain a gigaohm seal and thus to make ion channel recordings. Fig. 5 *C* shows a higher-resolution image of the one presented in Fig. 5 *B* where a successful patch clamp current recording was made of a channel located at the tip of a microvillus (*right panel*). This channel was identified as a K$^+$ channel on the basis of the reversal potential of the current-voltage curve under the experimental conditions used. Similar K$^+$ channels in A6 cells were previously described (Nilius et al., 1995). The probability of obtaining a seal by scanning patch clamp was 0.64 on the top of the microvillus (in a total of 25 patches). We were also able to patch between microvilli. We have previously been able to show that Cl$^-$ channels are also located at the top of microvilli in aldosterone-stimulated A6 cells, and it has also been suggested that other channel types are located here (Smith et al., 1997).

SUMMARY

We have demonstrated that the smart-patch approach can be used to make single-channel recordings from a large variety of preparations and to direct the patch pipette to precise

locations on cellular or subcellular structures. The implementation of the SICM feedback control by itself eases many of the technical problems associated with sealing patch pipettes on target cells, particularly when using very fine pipettes. Because the SICM protocols are well suited for use with pipettes that are much smaller than those conventionally used in patch-clamp recording, our method is a natural way to make recordings from small and precisely located areas of membrane. Furthermore, these structures need not be visible by light microscopy, and indeed opaque samples can be dealt with easily. Although very small pipettes do not have to be used for the smart-patch method, they do provide the highest-resolution images. The pipettes we use, having a diameter of ~200 nm, will sample an area of membrane that is only ~0.03 μm^2. However, we have shown that in a variety of preparations, channels can be detected and patch recordings made, because ion channels do not distribute evenly over the cell surface of the cell but cluster in specific subcellular locations.

Potential applications of the smart-patch technique and the use of its feedback control are quite varied. It can be applied to small cells such as sperm cells or to subcellular structures such as microvilli. It can be used to study nontransparent cell samples such as intact tissues, brain slice preparations, epithelial cultures, and hair cells. The spatial precision of the method allows a much improved ability to examine the special localization of ion channels, and the feedback system opens up the possibility of automated patch recording with possible applications in drug screening.

As the microscope nanopipette probe can be used to deliver defined chemical, electrical, or mechanical stimuli to precisely selected areas on the cell surface, this technique could, in the future, also be adapted to investigate the distribution of ligand-gated or mechano-gated ion channels or the effects of localized drug application.

REFERENCES

Alkondon, M., P. E. A. E.P. E. A. E. 1996. Mapping the location of functional nicotinic and gamma-aminobutyric acidA receptors on hippocampal neurons. *J. Pharmacol. Exp. Ther.* 279:1491–15061.

Angelides, K. J. 1986. Fluorescently labelled Na$^+$ channels are localized and immobilized to synapses of innervated muscle fibres. *Nature.* 321: 63–66.

Banke, T. G., A. Schousboe, and D. S. Pickering. 1997. Comparison of the agonist binding site of homomeric, heteromeric, and chimeric GluR1(o) and GluR3(o) AMPA receptors. *J. Neurosci. Res.* 49:176–185.

Carl, S. L., K. Felix, A. H. Caswell, N. R. Brandt, W. J. Ball, Jr., P. L. Vaghy, G. Meissner, and D. G. Ferguson. 1995. Immunolocalization of sarcolemmal dihydropyridine receptor and sarcoplasmic reticular triadin and ryanodine receptor in rabbit ventricle and atrium. *J. Cell Biol.* 129:672–682.

Cheng, H., M. B. Cannell, and W. J. Lederer. 1994. Propagation of excitation-contraction coupling into ventricular myocytes. *Pflugers Arch.* 428:415–417.

Cohen, M. W., O. T. Jones, and K. J. Angelides. 1991. Distribution of Ca^{2+} channels on frog motor nerve terminals revealed by fluorescent omega-conotoxin. *J. Neurosci.* 11:1032–1039.

Delmas, P., F. C. Abogadie, N. J. Buckley, and D. A. Brown. 2000. Calcium channel gating and modulation by transmitters depend on cellular compartmentalization. *Nat. Neurosci.* 3:670–678.

Dunn, P. M. 1994. Dequalinium, a selective blocker of the slow afterhyperpolarization in rat sympathetic neurones in culture. *Eur. J. Pharmacol.* 252:189–194.

Fan, J. S., Y. Yuan, and P. Palade. 2000. Kinetic effects of FPL 64176 on L-type Ca^{2+} channels in cardiac myocytes. *Naunyn Schmiedebergs Arch. Pharmacol.* 361:465–476.

Frosch, M. P., and M. A. Dichter. 1992. Non-uniform distribution of GABA activated chloride channels in cultured cortical neurons. *Neurosci. Lett.* 138:59–62.

Gu, Y., J. Gorelik, H. A. Spohr, A. Shevchuk, M. J. Lab, S. E. Harding, I. Vodyanoy, D. Klenerman, and Y. E. Korchev. 2002. High-resolution scanning patch-clamp: new insights into cell function. *FASEB J.* 16: 748–750.

Guerrero, A., J. A. Sanchez, and A. Darszon. 1987. Single-channel activity in sea urchin sperm revealed by the patch-clamp technique. *FEBS Lett.* 220:295–298.

Hamill, O. P., A. Marty, E. Neher, B. Sakmann, and F. J. Sigworth. 1981. Improved patch-clamp techniques for high-resolution current recording from cells and cell-free membrane patches. *Pflugers Arch.* 391:85–100.

Hansma, P. K., B. Drake, O. Marti, S. A. Gould, and C. B. Prater. 1989. The scanning ion-conductance microscope. *Science.* 243:641–643.

Harding, S. E., G. Vescovo, M. Kirby, S. M. Jones, J. Gurden, and P. A. Poole-Wilson. 1988. Contractile responses of isolated rat and rabbit myocytes to isoproterenol and calcium. *J. Mol. Cell. Cardiol.* 20: 635–647.

Hasbani, M. J., M. L. Schlief, D. A. Fisher, and M. P. Goldberg. 2001. Dendritic spines lost during glutamate receptor activation reemerge at original sites of synaptic contact. *J. Neurosci.* 21:2393–2403.

Joe, E. H., and K. Angelides. 1992. Clustering of voltage-dependent sodium channels on axons depends on Schwann cell contact. *Nature.* 356:333–335.

Johnston, D., J. C. Magee, C. M. Colbert, and B. R. Cristie. 1996. Active properties of neuronal dendrites. *Annu. Rev. Neurosci.* 19:165–186.

Jonas, E. A., R. J. Knox, and L. K. Kaczmarek. 1997. Giga-ohm seals on intracellular membranes: a technique for studying intracellular ion channels in intact cells. *Neuron.* 19:7–13.

Karpen, J. W., D. A. Loney, and D. A. Baylor. 1992. Cyclic GMP-activated channels of salamander retinal rods: spatial distribution and variation of responsiveness. *J. Physiol. (Lond.).* 448:257–274.

Kinnamon, S. C., V. E. Dionne, and K. G. Beam. 1988. Apical localization of K$^+$ channels in taste cells provides the basis for sour taste transduction. *Proc. Natl. Acad. Sci. U.S.A.* 85:7023–7027.

Korchev, Y. E., C. L. Bashford, M. Milovanovic, I. Vodyanoy, and M. J. Lab. 1997. Scanning ion conductance microscopy of living cells. *Biophys. J.* 73:653–658.

Korchev, Y. E., J. Gorelik, M. J. Lab, E. V. Sviderskaya, C. L. Johnston, C. R. Coombes, I. Vodyanoy, and C. R. Edwards. 2000b. Cell volume measurement using scanning ion conductance microscopy. *Biophys. J.* 78:451–457.

Korchev, Y. E., Y. A. Negulyaev, C. R. Edwards, I. Vodyanoy, and M. J. Lab. 2000a. Functional localization of single active ion channels on the surface of a living cell. *Nat. Cell Biol.* 2:616–619.

Lee, H. C. and D. L. Garbers. 1986. Modulation of the voltage-sensitive Na$^+$/H$^+$ exchange in sea urchin spermatozoa through membrane poten-

tial changes induced by the egg peptide speract. *J. Biol. Chem.* 261: 16026–16032.

Levitan, E. S. and R. H. Kramer. 1990. Neuropeptide modulation of single calcium and potassium channels detected with a new patch clamp configuration. *Nature.* 348:545–547.

Lievano, A., E. C. Vega-SaenzdeMiera, and A. Darszon. 1990. Ca^{2+} channels from the sea urchin sperm plasma membrane. *J. Gen. Physiol.* 95:273–296.

Lipscombe, D., D. V. Madison, M. Poenie, H. Reuter, R. Y. Tsien, and R. W. Tsien. 1988. Spatial distribution of calcium channels and cytosolic calcium transients in growth cones and cell bodies of sympathetic neurons. *Proc. Natl. Acad. Sci. U.S.A.* 85:2398–2402.

Munoz-Garay, C., J. L. Vega-Beltran, R. Delgado, P. Labarca, R. Felix, and A. Darszon. 2001. Inwardly rectifying K(+) channels in spermatogenic cells: functional expression and implication in sperm capacitation. *Dev. Biol.* 234:261–274.

Neher, E. and B. Sakmann. 1976. Single-channel currents recorded from membrane of denervated frog muscle fibres. *Nature.* 260:799–802.

Neher, E., B. Sakmann, and J. H. Steinbach. 1978. The extracellular patch clamp: a method for resolving currents through individual open channels in biological membranes. *Pflugers Arch.* 375:219–228.

Nilius, B., J. Sehrer, P. De Smet, W. Van Driessche, and G. Droogmans. 1995. Volume regulation in a toad epithelial cell line: role of coactivation of K^+ and Cl^- channels. *J. Physiol.* 487:367–378.

Park, J. S., M. C. Bateman, and M. P. Goldberg. 1996. Rapid alterations in dendrite morphology during sublethal hypoxia or glutamate receptor activation. *Neurobiol. Dis.* 3:215–227.

Sanchez, D., P. Labarca, and A. Darszon. 2001. Sea urchin sperm cation-selective channels directly modulated by cAMP. *FEBS Lett.* 503: 111–115.

Sariban-Sohraby, S., M. B. Burg, and R. J. Turner. 1984. Aldosterone-stimulated sodium uptake by apical membrane vesicles from A6 cells. *J. Biol. Chem.* 259:11221–11225.

Serrano, C. J., C. L. Trevino, R. Felix, and A. Darszon. 1999. Voltage-dependent Ca(2+) channel subunit expression and immunolocalization in mouse spermatogenic cells and sperm. *FEBS Lett.* 462:171–176.

Shevchuk, A., J. Gorelik, S. Harding, M. Lab, D. Klenerman, and Y. Korchev. 2001. Simultaneous measurement of Ca^{2+} and cellular dynamics: combined scanning ion conductance and optical microscopy to study contracting cardiac myocytes. *Biophys. J.* 81:1759–1764.

Smith, P. R., A. L. Bradford, S. Schneider, D. J. Benos, and J. P. Geibel. 1997. Localization of amiloride-sensitive sodium channels in A6 cells by atomic force microscopy. *Am. J. Physiol.* 272:C1295–C1298.

Stuart, G. J., H. U. Dodt, and B. Sakmann. 1993. Patch-clamp recordings from the soma and dendrites of neurons in brain slices using infrared video microscopy. *Pflugers Arch.* 423:511–518.

Sun, X. H., F. Protasi, M. Takahashi, H. Takeshima, D. G. Ferguson, and C. Franzini-Armstrong. 1995. Molecular architecture of membranes involved in excitation-contraction coupling of cardiac muscle. *J. Cell Biol.* 129:659–671.

Tousson, A., C. D. Alley, E. J. Sorscher, B. R. Brinkley, and D. J. Benos. 1989. Immunochemical localization of amiloride-sensitive sodium channels in sodium-transporting epithelia. *J. Cell Sci.* 93:349–362.